

Generation of Low Frequency Plasma Waves After Wave-Breaking

Prabal Singh Verma*

CNRS/Université d'Aix-Marseille Centre saint Jérôme,

case 232, F-13397 Marseille cedex 20, France

(Dated: May 25, 2022)

Abstract

Spatio-temporal evolution of a non-relativistic electrostatic waves in a cold plasma has been studied in the wave-breaking regime using a 1D particle-in-cell simulation. It is found that plasma gets heated after the wave-breaking but a fraction of initial energy always remains with the remnant wave in the form of BGK mode in warm plasma. An interesting finding of this work is that the frequency of the resultant BGK wave is found be below electron plasma frequency which decreases with increasing initial amplitude. Moreover, the acceleration mechanism after the wave-breaking is also found to be different from the previous work. In order to explain the results observed in the numerical experiments, a simplified theoretical model is constructed which exhibits a good agreement with the simulation. These investigations have direct relevance in wake-field acceleration experiments.

PACS numbers:

* prabal-singh.verma@univ-amu.fr

I. INTRODUCTION

Breaking of electrostatic waves [1–6] in plasma has a wide range of application from wake-field acceleration [7–10] to plasma heating in nuclear fusion experiments [11]. The phenomenon of wave-breaking was originally introduced by Dawson [1] using a sheet model in the cold plasma approximation where thermal corrections have been ignored. Considering ions which are much more massive than electrons fixed in space, Dawson has shown that as long as amplitude of the perturbation is small, oscillations stay linear and electron sheets oscillate coherently at electron plasma frequency. However, at larger amplitudes frequency of the oscillations remains the same but a peak in the electron density and corresponding steepening in the electric field profile starts to emerge as a nonlinear feature of the electron-plasma oscillations. At the critical amplitude (wave-breaking amplitude) electron density peak theoretically goes to infinity and coherent electrostatic energy starts to convert into random kinetic energy. It was predicted that all the electrostatic energy would get converted into random kinetic energy once the coherent oscillations are broken [1, 2]. In contrast it was shown in the previous work that a fraction of energy always remains with the wave as a superposition of two BGK-modes [12]. These modes form dynamically over several plasma periods after the breaking of standing cold plasma oscillations initiated by a sinusoidal density perturbations for $\delta n_e/n_0 > 0.5$.

The present work aims at investigating the behaviour of nonlinear plasma waves in the wave breaking regime because this configuration is more interesting from the application point of view. These waves can be excited in the wake of the laser pulse when it propagates into the plasma, provided frequency of the laser pulse matches the electron-plasma frequency [13]. Note here that when the group velocity of the laser pulse is close to speed of light, the wake waves are described by the time stationary solution of the relativistic electron fluid equations [14–17]. However, if the the group velocity of the laser pulse is much smaller than speed of light, wake waves in principle are described by the time-stationary solution of nonrelativistic electron fluid equations [3, 4, 18]. An exact time-stationary solution for such nonlinear waves has been first suggested by Davidson and Schram [3, 4]. These waves are also known as cold plasma BGK modes which can be obtained from the Lagrange solution too, for an unique choice of initial conditions [18]. When the maximum velocity amplitude of these waves becomes greater than or equal to the phase velocity ω_{pe}/k , wave-breaking

occurs due to the trajectory crossing between neighbouring oscillating electrons forming the wave and destroys the coherent motion. Therefore, from the wake-field acceleration point of view it is interesting to investigate what happens to these modes after they are broken. Do they also form coherent structures after the wave breaking as shown in the previous work for the case of standing oscillations ? If it is so, what kind of distribution functions are formed ? And most importantly what is the acceleration mechanism that allows the wave to capture and accelerate slower particles in order to loose coherent energy ? Note that in the case of standing plasma oscillation different ‘ k ’ modes have different phase velocities which were playing the main role in the acceleration process after the wave-breaking [12]. However, that is not the case for traveling waves because here all the ‘ k ’ modes propagate with same phase velocity $\sim \omega_{pe}/k$. Therefore, the aim of present work is to answer aforementioned questions in an effort to gain more insight into the physics of nonlinear plasma waves in the wave-breaking regime during their spatio-temporal evolution.

We use one dimensional particle-in-cell (1D PIC) simulations [19] to study the space-time evolution of cold plasma BGK wave [3, 4, 18] in the wave-breaking regime and find that the plasma gets heated after the wave-breaking but all the coherent energy does not vanish completely as a fraction of it always remains with the wave in the form of a single BGK mode in warm plasma [20, 21]. Although, the result is consistent with the previous finding [12], interestingly, the frequency of the final BGK wave is found to be below electron plasma frequency which decreases with increasing initial amplitude. Besides, the acceleration mechanism after the wave-breaking is also found to be very different from previous work [12]. In order to provide an understanding of this behaviour we construct a simplified theoretical model which shows a good agreement with numerical results.

The paper is organized as follows. Section II contains results from the simulation. In section III, interpretation of the numerical results is provided and section IV describes the theoretical modeling. Section V contains the summary and discussion of all the results presented in this paper.

II. RESULTS FROM THE SIMULATION

Here we carry out 1-D PIC simulation [19] with periodic boundary conditions, in order to study the evolution of large amplitude cold plasma BGK modes [3, 4, 18] beyond the wave

breaking amplitude. Our simulation parameters are as follows: total number of particles (N) $\sim 4 \times 10^4$, number of grid points (NG) $\sim 4 \times 10^3$, time step $\Delta t \sim \pi/50$. Ions are assumed to be infinitely massive which are just providing the neutralizing background to the electrons. Normalization is as follows. $x \rightarrow kx$, $t \rightarrow \omega_{pe}t$, $n_e \rightarrow n_e/n_0$, $v_e \rightarrow v_e/(\omega_{pe}k^{-1})$ and $E \rightarrow keE/(m\omega_{pe}^2)$, where ω_{pe} is the plasma frequency and k is the wave number of the longest (fundamental) mode. System length is $L = 2\pi$, therefore $k = 1$. The cold plasma BGK modes are initiated in the simulation by the following set of initial conditions,

$$\xi = kA \cos kx_{eq}, v_e = \omega_{pe}k^{-1}A \sin kx_{eq}, \quad (1)$$

where ξ is the initial displacement from the equilibrium position (x_{eq}) of the electrons, v_e is the initial velocity and ‘ A ’ is the amplitude of the perturbation. When ‘ A ’ is kept below 1, these initial conditions lead to propagating cold BGK-waves at the phase velocity $\omega_{pe}/k \sim 1$. As an example, we choose a case when $A = 1.05$ which is slightly beyond the critical (breaking) amplitude. In figures 1-10 we show snap-shots of phase space at various at time from $\omega_{pe}t = \pi/2$ to $\omega_{pe}t = 151\pi/2$.

At $A = 1.05$, electron-plasma wave starts to see some particle traveling close to its phase velocity, as a result these particles take energy from the wave and get accelerated to higher velocities as shown in figures 1-8. After approximately 25 plasma periods system reaches a stationary state because the phase space does not evolve any further as is shown in figures 9-10. In figures 11-12 we show the temporal evolution of averaged electrostatic energy (ESE) and averaged kinetic energy (KE) respectively. This evolution is found to be consistent with the phase space evolution as ESE initially decreases and later (approximately after 25 plasma periods) saturates at a finite amplitude. These results are found to be consistent with the previous study [12] as after the breaking of cold plasma BGK modes all the coherent energy does not vanish but some fraction always remains with the wave.

However, when we look at the distribution function in figure 13 at $\omega_{pe}t = 195\pi/2$, a flattening about $v = 0.5\omega_{pe}k^{-1}$ is noticed. This indicates that frequency of the remnant BGK-wave is much smaller than the electron plasma frequency ω_{pe} which is further confirmed from the fast Fourier transform (FFT) of the temporal evolution of the electric field at a fixed point in space, as is shown in figure 14. Moreover, it is also observed that frequency of the remnant BGK-wave decreases with increasing initial perturbation amplitude ‘ A ’ as is shown in figure 15. This behaviour is contrary to the previous work [12] where frequencies

of the remnant waves were never found to be below electron plasma frequency.

Since, the distribution function acquires a finite width in the stationary state, this indicates that plasma gets heated due to wave-breaking. The effective temperature is measured numerically by calculating the second moment of the final distribution function, which gives the root mean square speed v_{rms} of the particles, and define an effective thermal velocity v_{th} of the particles, which is found to be $\sim 1.0113\omega_{pe}k^{-1}$. We have also measured the temperature of fast and slow electrons (electrons supporting the wave) separately and it is found that the temperature of the slow electrons remains more or less same (corresponding thermal velocity $\sim 0.35\omega_{pe}k^{-1}$), however, temperature of the fast electrons increases with increasing initial amplitude ‘ A ’ as we see in figure 16.

In figure 17 we show the final electric field as a function of initial amplitudes which indicates that amplitude of the saturated electric field decreases much faster at comparatively smaller initial amplitudes. Note here that we are unable to compare the amplitude of final electric field with Coffey’s theoretical expression [22, 23] of maximum electric field in warm plasma because $v_{th}/v_{ph} > 1$ and this gives imaginary values when used in Coffey’s expression.

In the next section we provide a physical interpretation of the numerical experiments.

III. INTERPRETATION OF THE RESULTS

At an amplitude $A = 1.05$ even at $\omega_{pe}t = 0$ the cold BGK wave is able to see some electrons with velocities close to its phase velocity (~ 1). Therefore, it traps and accelerates them to high energies within one plasma period as we see in figures 1-2. We call these high energetic electrons as fast electrons because they do not oscillate at the electron-plasma frequency and their velocities are higher than the phase velocity of the cold plasma wave ($\sim \omega_{pe}/k$). These fast electrons give rise to a mean drift velocity along the $+x$ -direction. Note here that there is no net acceleration along the opposite direction which can cancel out the latter mean drift velocity. Therefore, in order to conserve the total momentum, rest of the plasma which is oscillating coherently starts to acquire a mean drift along the $-x$ direction. However, from the linear dispersion relation it is well known that if we have a plasma wave propagating in the $+x$ -direction along with a mean drift in the $-x$ -direction (say, $-v_0$), phase velocity (and hence frequency ω) of the plasma wave reduces due to the Doppler effect, *i.e.* $\omega = \omega_{pe} - kv_0$. Thus an increase in the mean drift velocity of the fast

electrons introduces a negative shift in the frequency and hence in the phase velocity of the electron-plasma wave. This enables plasma wave to trap and accelerate comparatively slower (than $\sim \omega_{pe}/k$) particles to higher velocities and thereby further reducing the phase velocity, as is seen in figures 3-4. This process keeps going on until the amplitude of the accelerating field, which is decreasing as the electrostatic energy is being lost in accelerating electrons, becomes so small that it is no more able to increase the mean drift velocity of the fast electrons any further. Therefore, no more further reduction of the phase velocity. Although, in this process few electrons with wave frame kinetic energy less than the potential energy maxima get trapped in the potential well of the plasma wave, which can then exchange energy with the wave during trapped oscillations. Meanwhile, with the progress of time, the trapped particle distribution becomes a well phase mixed through nonlinear Landau damping [24] such that an asymptotic state is finally reached where the distribution function becomes stationary in its own frame and the ESE neither grows nor damps. This explains the saturation in the ESE and KE in figures 11-12 after a certain time. These states are known as BGK waves in warm plasma which are time-stationary solutions of Vlasov-Poisson system [20, 21, 25] and the amplitude of such wave depends on the plateau Δv_{trap} , the width over which electrons are trapped in the wave trough which, in the normalized unit, is given by $\Delta v_{trap} = 2\sqrt{(2\phi)}$. In this case, Δv_{trap} is approximately 1.68 which is measured from figures 11-12 and amplitude of the wave potential ϕ is 0.357 which together satisfy the above mentioned theoretical expression quite accurately.

Note here that in the previous work [12] we have studied the breaking of standing plasma waves where no decrease in the frequency of the remnant waves was observed because there were fast electrons drifting in both $\pm x$ -directions thereby annihilating the net drifting effect on the frequency of the plasma oscillations.

In the next section we construct a simplified theoretical model in order to gain more insight into the numerical results.

IV. THEORETICAL MODEL

In the stationary state we have two kind of electrons. Ones which are oscillating coherently, however the second ones are fast electrons drifting along the $+x$ -direction. These fast electrons are responsible for inducing a mean drift velocity along the $-x$ -direction in the

rest of the plasma such that total mean momentum remains zero so as to satisfy momentum conservation. One can write down a linear dispersion relation for such a system as follows,

$$1 - \frac{\omega_{p1}^2}{(\omega - kv_{01})^2} - \frac{\omega_{p2}^2}{(\omega - kv_{02})^2} = 0, \quad (2)$$

where ω_{p1} and ω_{p2} are the frequencies of the coherently oscillating electrons and fast electrons respectively and v_{01} , v_{02} are their respective mean drift velocities. Thermal corrections have been ignored here for simplicity. Note here that $v_{02} > \omega/k$ and $\omega_{p2}^2 < \omega_{p1}^2$ as the number of fast electrons being much smaller than the number of coherently oscillating electrons. Therefore, the third term can be dropped from equation (2) because it has a weaker contribution as compared to the second term. Equation (2) is therefore approximated as,

$$1 - \frac{\omega_p^2}{(\omega - kv_{01})^2} \approx 0, \text{ i.e. } \omega \approx \omega_p + kv_{01} \quad (3)$$

where $\omega_p \approx \omega_{p2}$ is the frequency of the cold plasma wave. Since v_{01} arises in order to balance the effect of v_{02} , it is always negative and increases for higher initial amplitudes. This explains why the remnant wave acquires a frequency below ω_{pe} and why it decreases with increasing initial amplitude. In figure 18 we provide a comparison between numerical results and scaling for the theoretical model which shows a good agreement between the two. Here v_{01} is measured as a mean velocity of the coherently oscillating electrons.

V. SUMMARY AND DISCUSSION

In this paper, we have studied the long time evolution of large amplitude non-relativistic cold plasma BGK waves in the wave breaking regime and found that the plasma gets warm after the wave-breaking, however a fraction of initial energy always remains with the wave in the form of BGK-modes in warm plasmas [20, 21]. These findings are in agreement with the previous work where breaking of large amplitude standing plasma oscillations was studied [12]. However, in contrary the frequency of the remnant BGK-wave has been found to be below electron-plasma frequency which decreases further with increasing initial amplitude. This is because the fast electrons which are generated after the wave-breaking acquire a mean drift in the direction of acceleration and this mean drift has been found to increase for larger initial amplitudes. In order to cancel out this effect so as to conserve the total momentum, bulk of the plasma (coherently oscillating electrons) acquires a negative mean

drift velocity. The latter drift velocity allows remnant wave to acquire a frequency well below electron plasma frequency. However, in the previous study the electrons were drifting in both $\pm x$ -direction thereby canceling out the drifting effect on the bulk of the plasma. Therefore, we have not observed any decrease in the frequency of the coherent plasma oscillations after the wave-breaking [12].

Furthermore, the acceleration process after the wave-breaking has also been found to be different from the previous study [12]. This is due to the fact that in the case of standing oscillations we do not have any particles with velocities close to the phase velocity $\sim \omega_{pe}/k$. But, soon after the wave-breaking some high ' k ' modes (with phase velocities much smaller than $\sim \omega_{pe}/k$) acquire a small amount of energy which they resonantly transfer to the comparatively much slower particles and accelerate them to comparatively higher velocities. With increased velocities these particles get an opportunity to resonantly interact with smaller ' k ' modes (which have comparatively higher energies) and get accelerated to further higher velocities (for more detailed description please refer [12]). However, in the present study we already have electrons with velocities close to $\sim \omega_{pe}/k$ from the beginning, so they get accelerated to much higher velocities with in a plasma period. And these accelerated electrons self-consistently introduce a negative shift in the frequency of the plasma wave so that it can resonantly interact and give energy to comparatively slower particles. This process keeps going on until a stationary state is reached.

In order to gain an insight into the physics of the observed results in the numerical experiments, we have provided a theoretical model based on linear dispersion relation which has shown a good agreement between the two. Note here that although the frequencies of these BGK-waves are below electron-plasma frequency ω_{pe} , they are not electron acoustic modes [26, 27] because these modes are being generated due to the Doppler effect not due to the shielding effect [27]. These modes seem to be similar to KEEN waves as reported in [28].

These investigations have direct relevance in particle acceleration experiments because we learn here that plasma waves get slower after the wave-breaking in order to conserve the momentum and this may also be true for relativistic wake wave-breaking [7].

[1] J. M. Dawson, Physical Review **113**, 383 (1959).

- [2] J.-G. Wang, G. Payne, and D. Nicholson, *Physics of Fluids B: Plasma Physics* **4**, 1432 (1992).
- [3] R. Davidson and P. Schram, *Nuclear Fusion* **8**, 183 (1968).
- [4] R. Davidson, Academic, New York (1972).
- [5] G. Rowlands, G. Brodin, and L. Stenflo, *Journal of Plasma Physics* **74**, 569 (2008).
- [6] G. Brodin and L. Stenflo, *Physics Letters A* **381**, 1033 (2017).
- [7] A. Modena, Z. Najmudin, A. Dangor, C. Clayton, K. Marsh, C. Joshi, V. Malka, C. Darrow, C. Danson, D. Neely, et al., *nature* **377**, 606 (1995).
- [8] J. Faure, Y. Glinec, A. Pukhov, S. Kiselev, S. Gordienko, E. Lefebvre, J.-P. Rousseau, F. Burgy, and V. Malka, *Nature* **431**, 541 (2004).
- [9] A. Caldwell, K. Lotov, A. Pukhov, and F. Simon, *Nature Physics* **5**, 363 (2009).
- [10] M. Litos, E. Adli, W. An, C. Clarke, C. Clayton, S. Corde, J. Delahaye, R. England, A. Fisher, J. Frederico, et al., *Nature* **515**, 92 (2014).
- [11] R. Kodama, P. Norreys, K. Mima, A. Dangor, R. Evans, H. Fujita, Y. Kitagawa, K. Krushelnick, T. Miyakoshi, N. Miyanaga, et al., *Nature* **412**, 798 (2001).
- [12] P. S. Verma, S. Sengupta, and P. Kaw, *Physical Review E* **86**, 016410 (2012).
- [13] P. Gibbon, *Short pulse laser interactions with matter* (World Scientific Publishing Company, 2004).
- [14] A. I. Akhiezer and R. Polovin, *Soviet Phys. JETP* **3** (1956).
- [15] E. Infeld and G. Rowlands, *Physical Review Letters* **62**, 1122 (1989).
- [16] P. S. Verma, S. Sengupta, and P. Kaw, *Physical Review Letters* **108**, 125005 (2012).
- [17] R. K. Bera, S. Sengupta, and A. Das, *Physics of Plasmas* **22**, 073109 (2015).
- [18] J. Albritton and G. Rowlands, *Nuclear Fusion* **15**, 1199 (1975).
- [19] C. K. Birdsall and A. B. Langdon, *Plasma physics via computer simulation* (CRC Press, 2004).
- [20] I. B. Bernstein, J. M. Greene, and M. D. Kruskal, *Physical Review* **108**, 546 (1957).
- [21] I. Hutchinson, *Physics of Plasmas* **24**, 055601 (2017).
- [22] T. Coffey, *The Physics of Fluids* **14**, 1402 (1971).
- [23] W. Mori and T. Katsouleas, *Physica Scripta* **1990**, 127 (1990).
- [24] T. O'neil, *The Physics of Fluids* **8**, 2255 (1965).
- [25] G. Manfredi, *Physical Review Letters* **79**, 2815 (1997).
- [26] N. Sircombe, T. Arber, and R. Dendy, *Plasma physics and controlled fusion* **48**, 1141 (2006).

- [27] N. Chakrabarti and S. Sengupta, *Physics of Plasmas* **16**, 072311 (2009).
- [28] T. Johnston, Y. Tyshetskiy, A. Ghizzo, and P. Bertrand, *Physics of Plasmas* **16**, 042105 (2009).

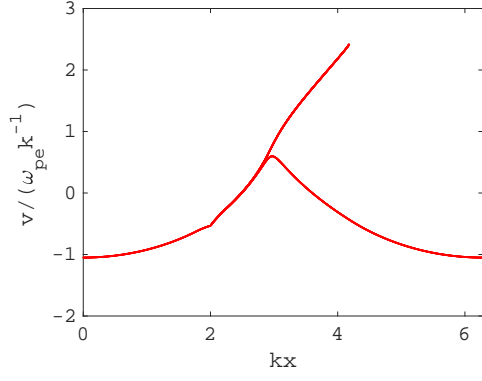


FIG. 1: Phase-space snap shot at $\omega_{pet} = \pi/2$ for $A = 1.05$.

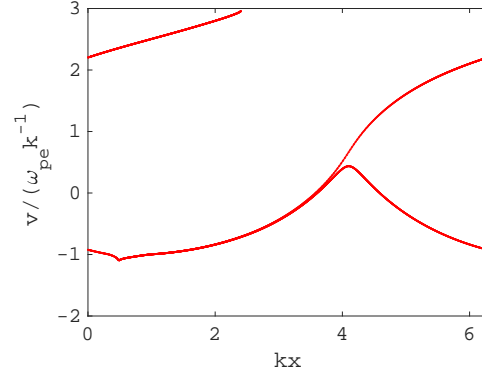


FIG. 2: Phase-space snap shot at $\omega_{pet} = \pi$ for $A = 1.05$.

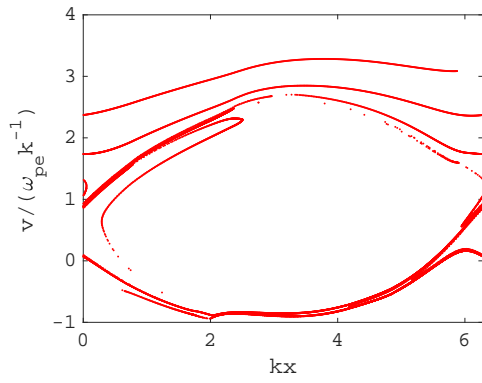


FIG. 3: Phase-space snap shot at $\omega_{pet} = 9\pi/2$ for $A = 1.05$.

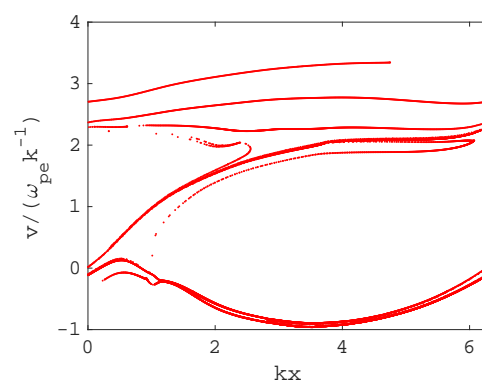


FIG. 4: Phase-space snap shot at $\omega_{pet} = 5\pi$ for $A = 1.05$.

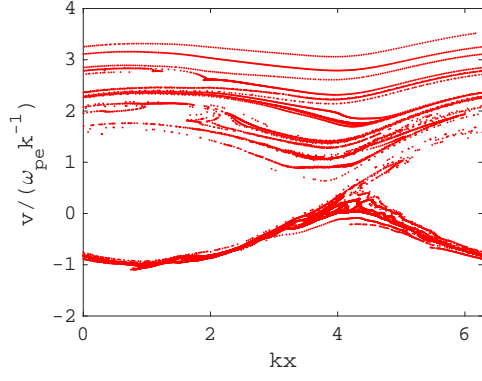


FIG. 5: Phase-space snap shot at $\omega_{pet} = 21\pi/2$ for $A = 1.05$.

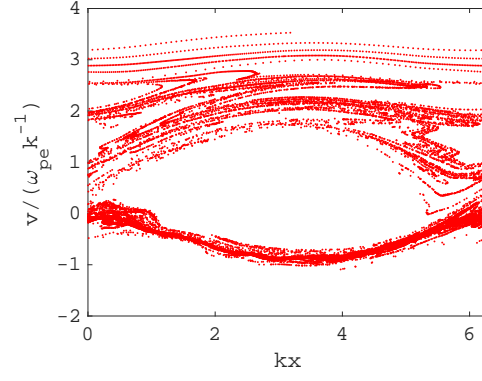


FIG. 6: Phase-space snap shot at $\omega_{pet} = 31\pi/2$ for $A = 1.05$.

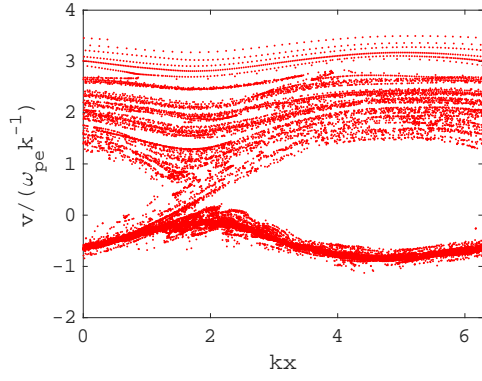


FIG. 7: Phase-space snap shot at $\omega_{pet} = 41\pi/2$ for $A = 1.05$.

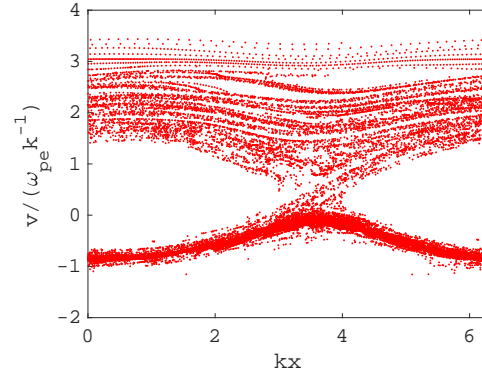


FIG. 8: Phase-space snap shot at $\omega_{pet} = 51\pi/2$ for $A = 1.05$.

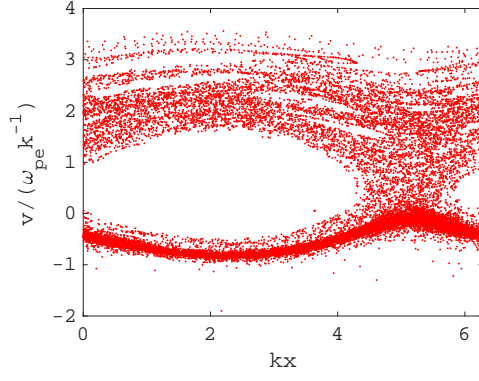


FIG. 9: Phase-space snap shot at $\omega_{pe}t = 101\pi/2$ for $A = 1.05$.

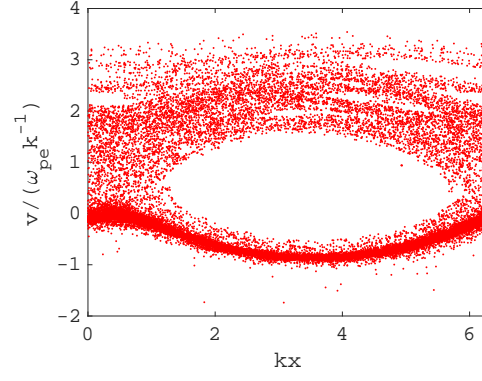


FIG. 10: Phase-space snap shot at $\omega_{pe}t = 151\pi/2$ for $A = 1.05$.

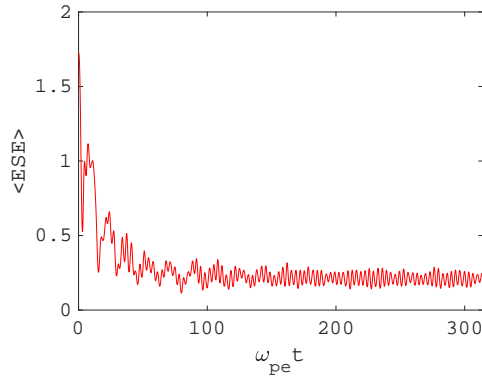


FIG. 11: Temporal evolution of averaged electrostatic energy $\langle ESE \rangle$ for $A = 1.05$.

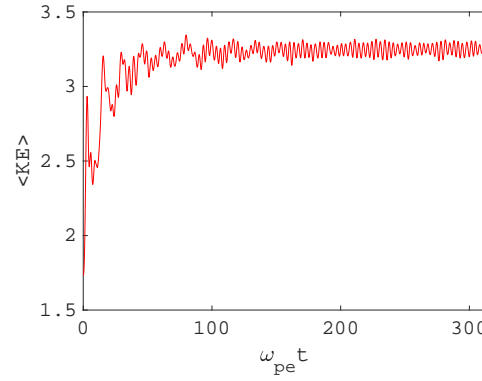


FIG. 12: Temporal evolution of averaged kinetic energy $\langle KE \rangle$ for $A = 1.05$.

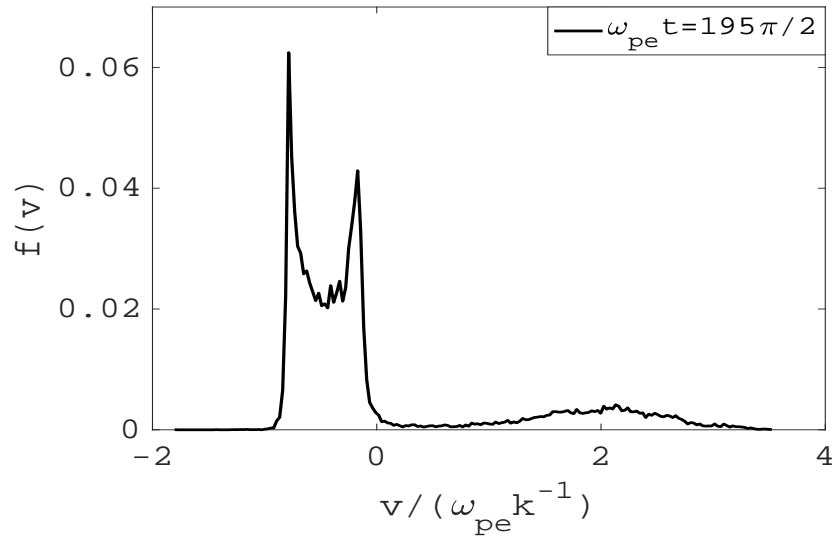


FIG. 13: Distribution function at $\omega_{pe}t = 195\pi/2$ for $A = 1.05$.

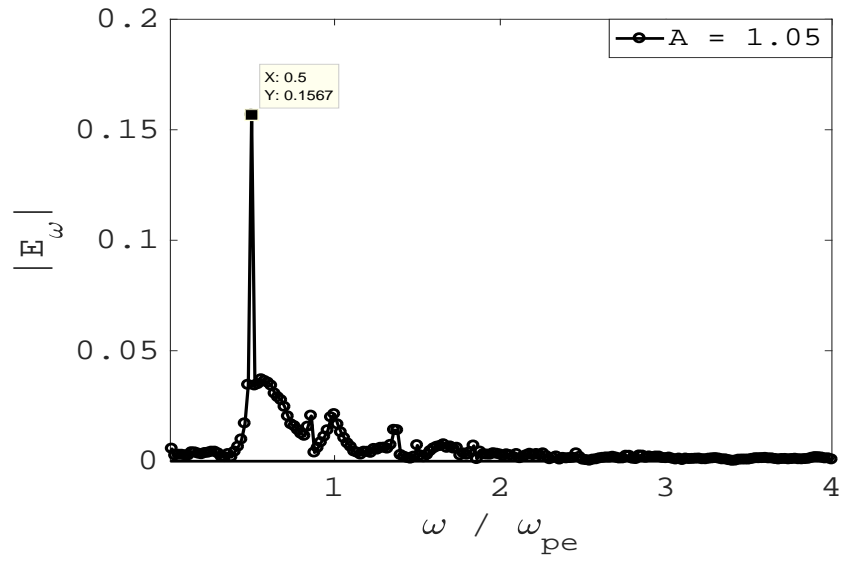


FIG. 14: FFT of the temporal profile of the electric field for $A = 1.05$.

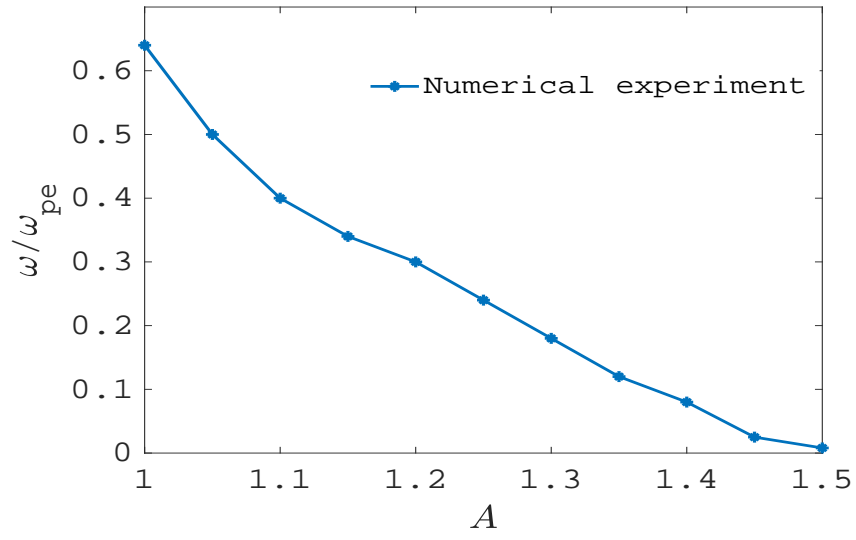


FIG. 15: Frequency of the remnant BGK wave versus initial amplitude at $\omega_{pe}t = 195\pi/2$.

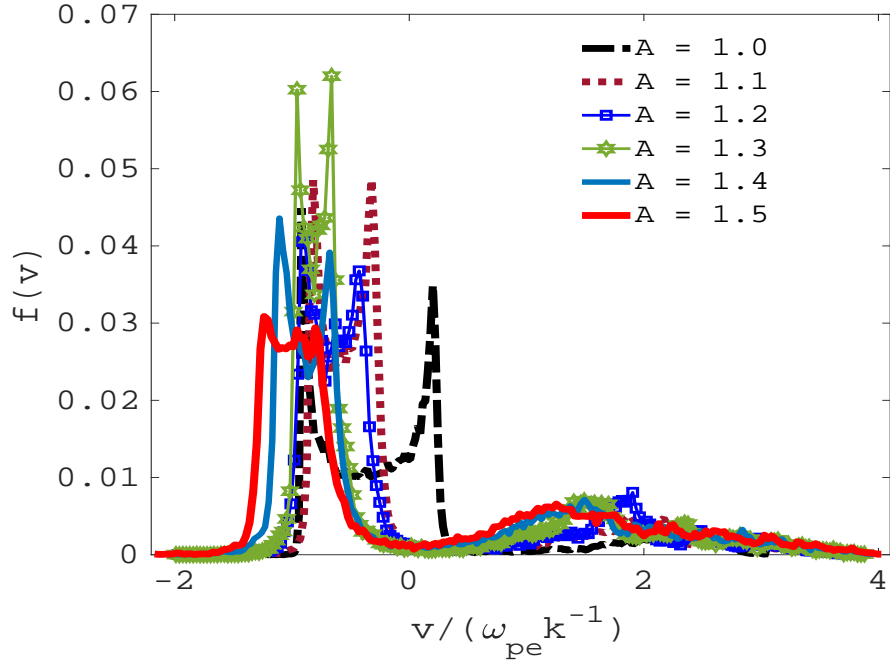


FIG. 16: Distribution functions for different initial amplitudes at $\omega_{pe}t = 195\pi/2$.

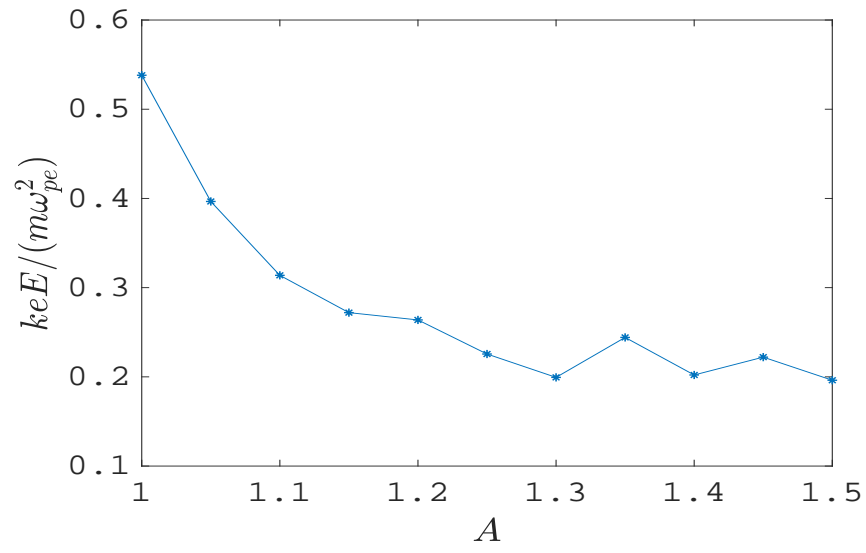


FIG. 17: Amplitude of the saturated electric field as a function of initial amplitude at $\omega_{pe}t = 195\pi/2$.

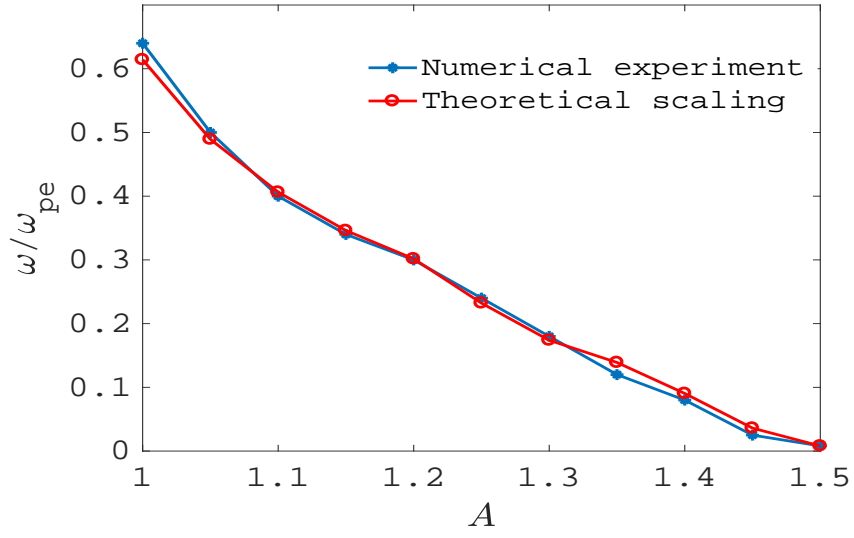


FIG. 18: Frequency of the remnant BGK wave (ω) as function of initial amplitude ‘A’ – a comparison between numerical experiment (blue line points) and theoretical scaling (red line points).